High Gain Direct Drive Target Designs and Supporting Experiments with KrF[*)]

Max KARASIK, Yefim AGLITSKIY[1)], Jason W. BATES, Denis G. COLOMBANT[4)], David M. KEHNE, Wallace M. MANHEIMER[2)], Nathan METZLER[2,3)], Jaechul OH[2)], Andrew J. SCHMITT, Victor SERLIN, Alexander L. VELIKOVICH, James L. WEAVER, Steven T. ZALESAK[4)] and Stephen P. OBENSCHAIN

Plasma Physics Division, Naval Research Laboratory, 4555 Overlook Ave, SW, Washington DC 20375, USA
[1)] *SAIC, McLean, VA 22150, USA*
[2)] *Research Support Instruments, Lanham, MD 20706, USA*
[3)] *Ben Gurion University, Beer Sheva, Israel*
[4)] *Berkeley Research Associates, Beltsville, MD 20705, USA*

(Received 1 June 2012 / Accepted 9 August 2012)

Krypton-fluoride laser is an attractive inertial fusion energy driver from the standpoint of target physics. Target designs taking advantage of zooming, shock ignition, and favorable physics with KrF reach energy gains of 200 with sub-MJ laser energy. The designs are robust under 2D simulations. Experiments on the Nike KrF laser support the physics basis.

Keywords: inertial fusion, fusion energy, krypton fluoride laser, direct drive, high gain, target design, laser-plasma instability, high velocity, hydrodynamics

DOI: 10.1585/pfr.8.3404042

1. Introduction

For a fusion power plant to be useful, the imploded target has to release enough energy to power the reactor and produce electricity for the grid. Higher gain (fusion energy released divided by driver energy) increases the power to the grid and reduces the fraction of power needed to operate the reactor (recirculating power fraction). Practical considerations suggest that the recirculating power fraction should not exceed 1/4 of the total power generated. This implies that the product of driver efficiency η and target gain G should be $\eta G \geq 10$.

Experiments, theoretical work, and simulations in laser fusion have been carried out at the Naval Research Laboratory (NRL) since the 1970's and in krypton-fluoride (KrF) lasers in particular since 1990's. Recent advances in target designs and KrF laser technology show a pathway to an attractive power plant driver with sub-MJ laser energy.

Achieving high gain implosions is challenging in a number of ways. Hydrodynamic instabilities can spoil implosion uniformity and prevent hot spot formation. Laser-plasma instabilities can reduce laser absorption and preheat the fuel, preventing compression to high density. Finally, coupling of laser energy to the target needs to be efficient in order to obtain high gain. Use of the deeper UV KrF laser light (λ = 248 nm) helps overcome these challenges. Deeper UV gives higher thresholds for laser-plasma instabilities, higher mass ablation rates and ablation pressure (allowing more stable lower aspect ratio targets), higher hydrodynamic efficiency, and higher absorption fraction. KrF laser architecture allows the use of induced spatial incoherence (ISI) smoothing technique, which together with its high bandwidth (up to 3 THz) produces the most uniform target illumination of all high energy lasers, minimizing laser imprint. Furthermore, the KrF focal profile can be zoomed down during the pulse to follow the imploding pellet, reducing the laser energy required by 30%.

These significant physics advantages are coupled with maturing rep-rate KrF laser technology. The 5 Hz, 700 J/pulse Electra KrF amplifier at NRL demonstrated 90,000 shots continuous operation (see paper by Wolford in this issue). Its operation points to a 7.1% wall-plug efficiency for a KrF power plant driver. With this efficiency and gains reaching 200, a sub-MJ KrF laser driver satisfies the $\eta G \geq 10$ requirement.

This paper is organized as follows. High gain target designs are presented in Sec. 2, example of supporting target physics experiments are given in Sec. 3 and 4, and conclusions are drawn in Sec. 5.

2. High Gain Target Designs Utilizing KrF

Direct drive [1] allows high energy gains by efficiently coupling laser energy to the target. Furthermore, direct drive allows a fast-rising, intense spike in drive pressure

author's e-mail: karasik@nrl.navy.mil

*) This article is based on the presentation at the Conference on Inertial Fusion Energy '12.

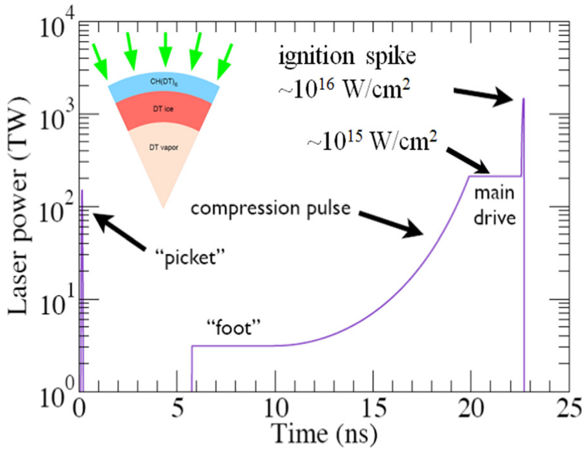

Fig. 1 Shock ignition pulseshape. Inset shows a sector of the pellet with layers: DT-wicked CH foam + DT ice + DT vapor.

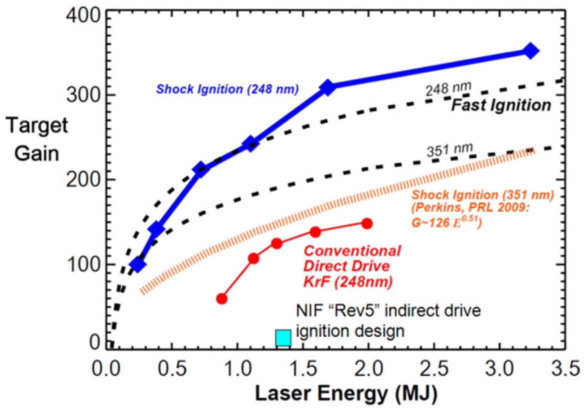

Fig. 2 Shock ignition gain is comparable to fast ignition. Fast ignition curves are based on Ref [3]. 351 nm shock ignition curve is based on Ref [4].

at the end of the pulse for shock ignition [2]. Direct drive ignition physics can be explored on the NIF by making use of polar direct drive and by reconfiguring the beams for spherically symmetric illumination. There are two laser driver options for direct drive: solid state frequency tripled laser (351 nm) and KrF gas laser (248 nm). Making use of zooming (shrinking the laser spot size to follow the imploding pellet) and higher ablation pressures available using the shorter wavelength (248 nm) KrF laser gives a significant decrease in the laser energy required. Shock ignition utilizing KrF raises the gain sufficiently for power plant operation (ηG>10) for a sub-MJ KrF driver.

2.1 Shock ignition designs

Shock ignition, similarly to fast ignition, provides a degree of separation between cold fuel assembly and hot spot formation. The pellet shell is accelerated to sub-ignition velocity (< 300 km/sec), and ignited by a converging shock produced by high intensity spike in the laser pulse (Fig. 1). Shock ignition gives gains comparable to fast ignition (Fig. 2) with fewer physics unknowns and without the need for a separate ignition laser.

The energy gain advantages of using zooming and shorter wavelength are illustrated in Table 1, which gives results of implosion simulations for three cases: 248 nm (KrF) with zooming, 351 nm (Nd:glass) with zooming, and 351 nm without zooming. The parameters were selected such that the yield is approximately equal for all three cases. The laser energy needed, however, varies significantly, resulting in large differences in gain. Moreover, peak compression intensity for the 351 nm cases was increased compared to the 248 nm case to keep the ablation pressure constant. If this increase results in unacceptable levels of laser-plasma instability (LPI), differences in laser energy needed would be even larger.

Table 1 Benefits from shorter λ and zooming.

	KrF λ=248 nm with Zoom	**Nd:glass** λ=351 nm with Zoom	**Nd:glass** λ=351 nm no Zoom
Laser Energy	**230 kJ**	**430 kJ**	**645 kJ**
Yield	22 MJ	24 MJ	23 MJ
Gain	**97**	**56**	**35**
Peak compression intensity (W/cm²)	1.5×10^{15}	2.2×10^{15}	1.9×10^{15}
Peak igniter intensity (W/cm²)	1.6×10^{16}	3.1×10^{16}	2.2×10^{16}

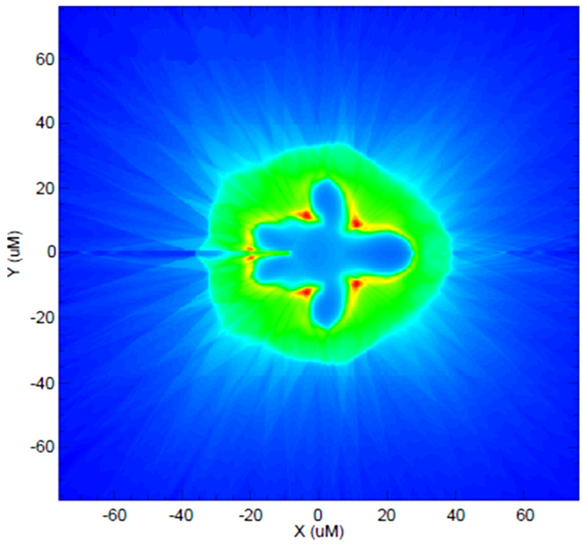

Fig. 3 Density image of a 2D high resolution (l = 1-256), 521 kJ KrF implosion with shock ignition at the time of peak ρR resulting in a gain of 102 (1D gain is 142). The simulation includes outer and inner surface roughness and ISI laser imprint.

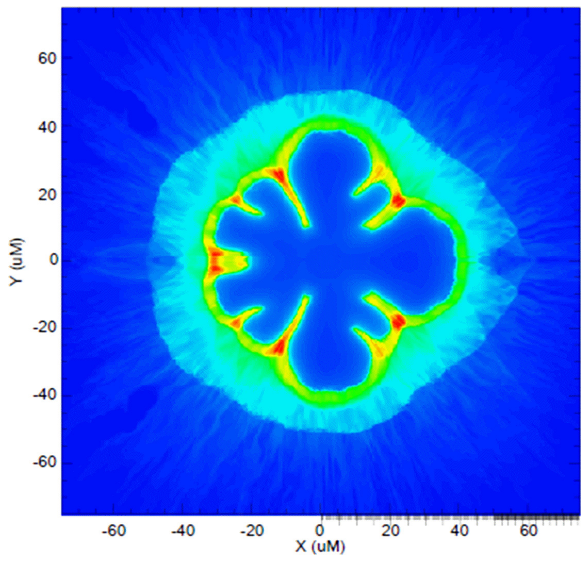

Fig. 4 A higher aspect ratio (3.7), 529 kJ KrF implosion with shock ignition resulting in a gain of 136. The simulation includes outer and inner surface roughness and ISI laser imprint.

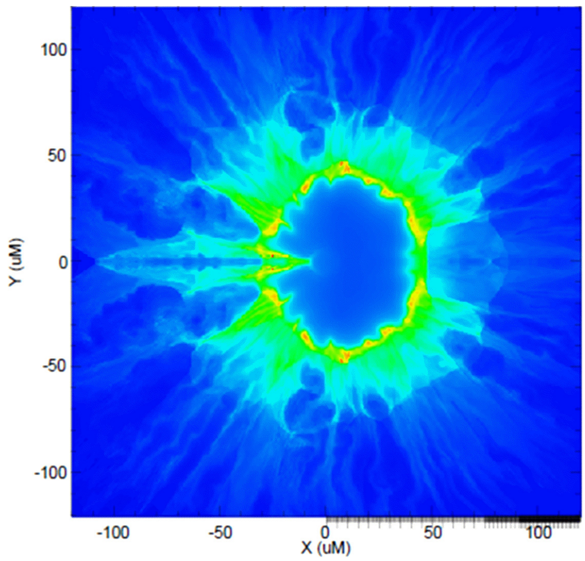

Fig. 5 Increasing initial aspect ratio too far can lead to target failure due to hydrodynamic instability: this aspect ratio 6.2 pellet fails to ignite.

2.2 High resolution 2D simulations

Because of the higher ablation pressure and higher LPI thresholds, KrF shock ignition designs can utilize lower aspect ratio targets, giving good hydro stability. High resolution 2D simulations using NRL's FASTrad3D code show that the high gain is retained in the presence of realistic target roughness and laser imprint (see Fig. 3).

2.3 Managing laser-plasma instability (LPI) risk

LPI and its impact for a full-scale target is not yet known, however the risk is lower for shorter laser wavelength. LPI risk can also be reduced by trading hydrodynamic stability for LPI suppression: increasing the initial aspect ratio of the target allows one to use lower drive intensities. From the simple scaling for LPI thresholds that has been observed in experiments so far (see Sec 4 below), the ratio of peak intensity during the target implosion to LPI intensity threshold decreases with aspect ratio. Though both the 351 nm and 248 nm designs are above threshold, the LPI risk for 248 nm is significantly lower. A high resolution 2D simulation with a higher aspect ratio is shown in Fig. 4. The fuel assembly is not as uniform as compared to lower aspect ratio (Fig. 3) target, but the high gain is retained.

Increasing the aspect ratio in order to decrease the drive intensity can only be taken so far before hydrodynamic instability causes the target to fail. Figure 5 shows a snapshot from a simulation of a low adiabat pellet driven by a low intensity pulse (peak intensity of compression pulse = 140 TW/cm^2) with an initial aspect ratio of 6.2. The pellet does not ignite.

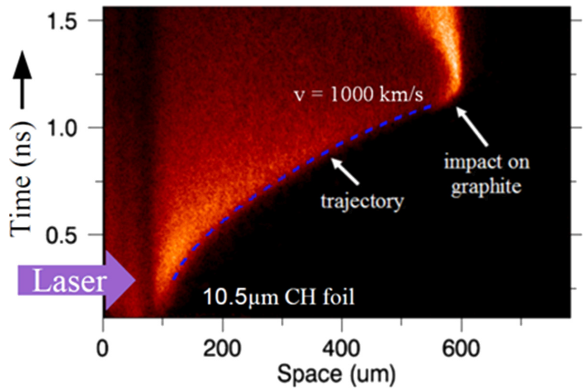

Fig. 6 Side-on x-ray image of an accelerating 10.5 μm CH target. The trajectory traced from the image is overlaid as a dashed line. The impact on a stationary foil marked by bright emission is clearly visible.

3. Hydrodynamics Experiments on Nike

Experiments on the Nike KrF laser allow basic studies of elements of ICF and provide a platform for benchmarking the simulations. Recent experiments on Nike took advantage of its ultra-high uniformity and higher ablation pressures to accelerate foils to record velocity of 1000 km/s and generate Gbar pressures on impact with a stationary foil (Fig. 6) [5]. Thermonuclear temperatures were produced in this planar impact, and, in the case of deuterated polystyrene, 10^6 fusion neutrons were produced with ion temperature measured to be 2-3 keV by neutron time-of-flight detectors.

Current target designs call for adiabat-shaping spikes

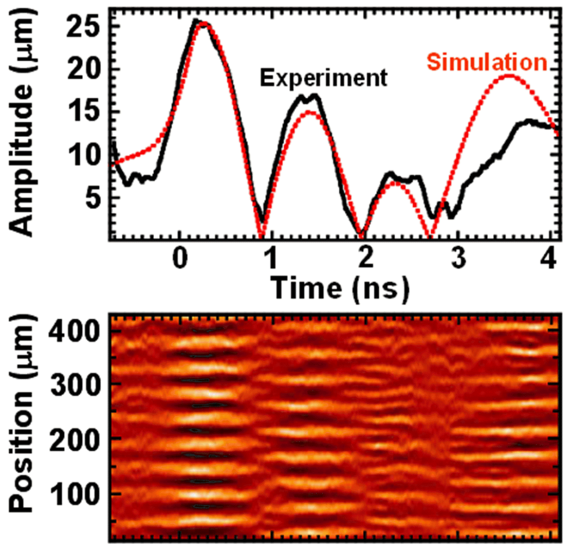

Fig. 7 Top: experimental (solid) and simulated (dotted line) time histories of the areal mass modulation amplitude in a 125 µm thick target with a 45 µm wavelength ripple. Bottom: areal mass perturbations in the range of 22 to 50 µm obtained from an x-ray streak radiograph of the target.

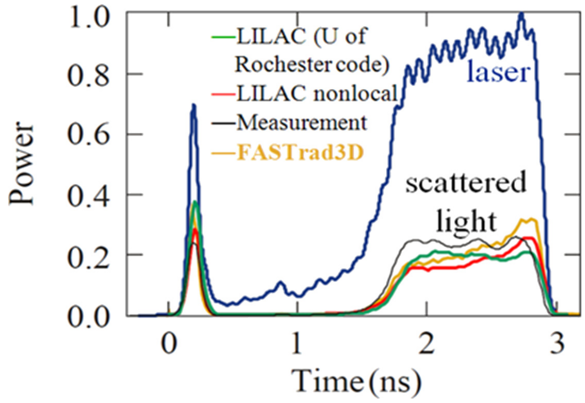

Fig. 8 Measurements of scattered light from Ref [7] simulated by University of Rochester's code and NRL's FASTrad3D code.

in the laser pulseshape, with an ignition spike at the end. In recent experiments on Nike, theoretically predicted large oscillations of the areal mass in the target following such a spike have been observed for the first time [6]. Multiple phase reversals of the areal mass modulation are detected (Fig. 7).

NRL's FASTrad3D radiation hydrodynamics code has also been benchmarked against experiments on the OMEGA laser at University of Rochester. Figures 8 and 9 show two examples: a simulation of backscattered light and a simulated implosion trajectory, respectively.

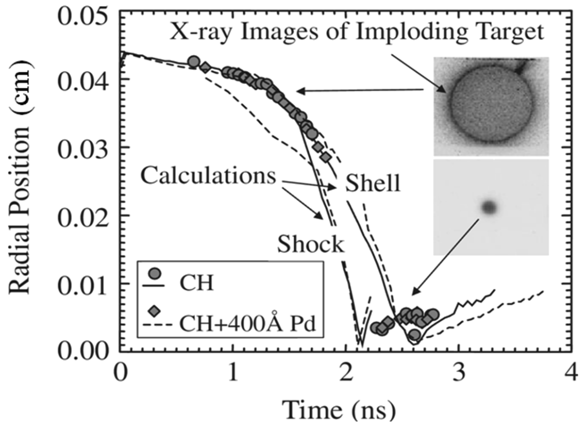

Fig. 9 Implosion trajectory simulated with FASTrad3D agrees with the measurements [9].

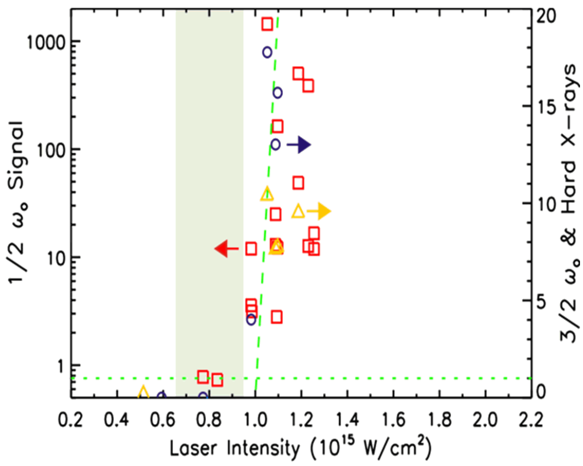

Fig. 10 Measurements are consistent with the simple threshold formula (shaded region) giving higher LPI thresholds for KrF lasers than for 351 nm lasers.

4. Laser-Plasma Instability Experiments on Nike

Numerous laser plasma instability experiments have been conducted for 351 nm and longer laser wavelengths (see for example Ref [8]). LPI experiments on Nike aim to extend these measurements to 248 nm. Measurements thus far are consistent with the simple formula for LPI thresholds, giving higher thresholds for KrF lasers than for 351 nm lasers: $I_{15\mathrm{thresh}} \approx 80T_{\mathrm{keV}}/\lambda_{\mu\mathrm{m}}L_{\mu\mathrm{m}}$ (Fig. 10).

5. Conclusions

Advances in direct drive high gain target designs point to power-plant relevant gains with smaller laser drivers. KrF laser is an attractive inertial fusion energy driver from the standpoint of target physics. Target designs taking advantage of zooming, shock ignition, and favorable physics with KrF reach energy gains of 200 with sub-MJ laser energy. High resolution 2D simulations show that the designs are robust against hydrodynamic instabilities, retaining the high gain. Experiments on the Nike KrF laser support the physics basis and offer an important platform for benchmarking the simulations.

Acknowledgement

This work is supported by the U.S. Department of Energy, NNSA Defense Programs.

[1] S.E. Bodner *et al.*, Phys. Plasmas **5**, 1901 (1998).
[2] R. Betti *et al.*, Phys. Rev. Lett. **98**, 155001 (2007).
[3] R. Betti, Phys. Plasmas **13**, 100703 (2006).
[4] L.J. Perkins *et al.*, Phys. Rev. Lett. **103**, 045004 (2009).
[5] M. Karasik *et al.*, Phys. Plasmas **17**, 056317 (2010).
[6] Y. Aglitskiy *et al.*, Phys. Rev. Lett. **109**, 085001 (2012).
[7] W. Seka *et al.*, Phys. Plasmas **15**, 056312 (2008).
[8] W. Seka *et al.*, Phys. Plasmas **16**, 052701 (2009).
[9] A.N. Mostovych *et al.*, Phys. Rev. Lett. **100**, 075002 (2008).